Content-State Dimensions Characterize Different Types of Neural Correlates of Consciousness

Pauline Perez* 1,2,3, Dragana Manasova* 1,4, Bertrand Hermann 1,4,5, Federico Raimondo 1,6,7, Benjamin Rohaut 1,3, Tristán A. Bekinschtein 8, Lionel Naccache 1,9, Anat Arzi 1,8, Jacobo D. Sitt 1

*** Co-first authors**

1 - Sorbonne Université, Institut du Cerveau - Paris Brain Institute - ICM, Inserm, CNRS, 75013, Paris, France

2 - Hospice Civils de Lyon - HCL, Département anesthésie-réanimation, Hôpital Edouard Herriot

3 - AP-HP, Hôpital de la Pitié Salpêtrière, Neuro ICU, DMU Neurosciences, Paris, France

4 - Université Paris Cité, Paris, France

5 - Medical intensive care unit, HEGP Hôpital, Assistance Publique - Hôpitaux de Paris-Centre (APHP-Centre), Paris, France

6 - Institute of Neuroscience and Medicine (INM-7: Brain and Behaviour), Research Centre Jülich, Germany

7 - Institute of Systems Neuroscience, Heinrich Heine University Düsseldorf, Germany

8 - Consciousness and Cognition Lab, Department of Psychology, University of Cambridge

9 - AP-HP, Hôpital Pitié-Salpêtrière, Service de Neurophysiologie Clinique, Paris, France

Correspondence: jacobo.sitt@icm-institute.org (J. D. Sitt)

Abstract

Identifying the neural correlates of consciousness (NCCs) is key to support the different scientific theories of consciousness. NCCs can be defined to reflect either the brain signatures underlying specific conscious content or those supporting different states of consciousness, two aspects traditionally studied separately. In this paper, we introduce a framework to characterize NCCs according to their dynamics in both the 'state' and 'content' dimensions. The two-dimensional space is defined by the NCCs' capacity to distinguish the conscious states from non-conscious states, (x-axis) and the content (perceived versus unperceived, y-axis). According to the sign of the x and y-axis, NCCs are separated into four quadrants in terms of how they distinguish the state and content dimensions. We implement the framework using three types of EEG NCCs: markers of connectivity, markers of complexity, and spectral summaries. The NCC-state is represented by the level of consciousness in 1) patients with disorders of consciousness; 2) healthy participants' during a nap. On the other hand NCC-content by the conscious content in healthy participants' perception tasks: 1) auditory local-global paradigm and 2) visual awareness paradigm. In both cases, we see separate clusters of NCCs with correlated and anti-correlated dynamics, shedding light on the complex relationship between the state and content of consciousness and emphasizing the importance of considering them simultaneously. This work presents an innovative framework for studying consciousness by examining NCC in a two-dimensional space, providing a valuable resource for future research, with potential applications using diverse experimental paradigms, neural recording techniques, and modeling investigations.

Keywords :

Consciousness, Sleep, Conscious content, Disorders of consciousness, Neural correlates of consciousness

Introduction

Giving a definition of consciousness with a coherent theoretical framework is a daunting task that would benefit from simple conceptual dissociations to improve interpretability. Identifying the neural correlates of consciousness (NCC) has become crucial to allow progress in the science of consciousness. Following the Koch & Crick seminal definition, neural correlates of consciousness are the minimal neural processes that must occur in the brain for a particular conscious experience to occur (Crick & Koch, 1990), however, this definition leaves the possibility of two types of NCC, those of conscious contents and those of states of consciousness.

Traditionally, research on consciousness has developed separately in these two pillars. While some researchers, mainly cognitive neuroscientists, primarily focused on the neuronal processes behind conscious access of specific content (e.g. the capacity to report stimuli as seen versus not seen, or to discriminate which stimuli). The second line of researchers focused on global states of consciousness (e.g. sleep, anesthesia, and disorders of consciousness) (Bayne et al., 2016; Boly et al., 2013; Sanders et al., 2012; Goupil and Bekinschtein; 2012). This research has been rather developed by physicians with questions of diagnosis and prognosis often sanctioned by ethical and end-of-life questions.

Neural correlates of conscious content (NCC-C) are a reflection of the neural processes that occur for a specific experience. NCC-C are normally studied by comparing conditions where specific conscious content (e.g. perception of sound or image) is present or absent while stimulus properties - and state of consciousness - remain unchanged. The difference between the neural activities averaged by trials depending on the capacity to report (reported perceived, eg. "seen"), compared to the lack of capacity to report (reported not perceived, eg. "not-seen") is generally considered to be a neural correlate of consciousness of content. Several different paradigms exist such as perceptual suppression, masking, or threshold paradigms in different sensory modalities (Del Cul et al., 2007, Dehaene & Changeux, 2011; Kim & Blake, 2005). In addition, there are tasks that assess the capacity to attend and integrate perceptual and cognitive irregularities such as the auditory local-global paradigm (Bekinschtein et al., 2009). Various methods such as EEG, MEG, or fMRI allow for studying the neural correlates of these conscious perceptual experiences (Koch et al., 2016; Tsuchiya et al., 2015). From these studies, the NCC-C which differentiates the “seen” from the “not-seen” range from the primary and secondary networks of early perceptual and cognitive integration to abstract cognitive implementation associative areas (Dehaene & Changeux, 2011). Electrophysiological studies on monkeys and humans have revealed several signatures of auditory awareness like P3b event related potentials and oscillations in α / β (9-30 Hz) and γ (> 40 Hz) bands between the visual cortex and frontoparietal cortices (Dehaene & Changeux, 2011). The auditory local-global paradigm was designed to specifically capture EEG potentials that are directly linked to the conscious processing of hierarchical regularities (Bekinschtein et al., 2009).

Neuronal Correlates of Conscious State (NCC-S) are used to differentiate states of consciousness. These include conditions as diverse as sleep, partial complex seizures, general anesthesia, and patients in a vegetative state or in a minimal consciousness state (Laureys et al., 2004). NCC-S can signal the emergence of consciousness, with the brain having to be at an appropriate level of processing to "ensure adequate cortical excitability" for the emergence of consciousness (Koch et al., 2016). Consciousness disorders in patients with brain injury are a good model of different states of consciousness as they provide a spectrum of conscious states. The current taxonomy to describe these patients is based on neurological evaluation (CRS-R, Coma Recovery Scale-Revised (Kalmar & Giacino, 2005)). This evaluation classifies these patients in different clinical conditions: the vegetative state patient (VS) - otherwise called unresponsive wakefulness syndrome (UWS) (Laureys et al., 2010), characterized by a behavioral examination of eyes open without awareness (Jennett & Plum, 1972). The second clinical condition is the minimally conscious state (MCS) (more recently proposed to be renamed as cortically mediated state (CMS) (Naccache 2018)), with patients showing reproducible behavioral responses suggesting environmental awareness such as slow visual pursuit or response to simple commands; and finally, the exit-MCS (EMCS) patient, able to maintain some degree of basic communication (Giacino et al., 2002). These three clinical categories can be considered 'ordered' in a gradient reflecting the richness of conscious experience (Bayne et al., 2016). These theoretical and behavioral findings are also verified - and in many cases enriched (Naccache, 2018) - by NCC-S. For example, different electrophysiological markers derived from EEG recording in a resting state (Sitt et al., 2014; Chennu et al., 2014) are able to discriminate VS/UWS patients from MCS patients. In the same way, fMRI during a resting state period (Demertzi et al.,

2014, 2015, 2019; Di Perri et al., 2016), PET with metabolic markers (Stender et al., 2014, Hermann et al., 2021) or the calculation of an index reflecting the EEG reaction after stimulation by TMS (Casarotto et al., 2016), are capable of discriminating between VS/UWS and MCS patients. This contrast makes it possible to study the VS/UWS as a state of wakefulness without awareness, and the MCS as a state with minimal behaviors consistent with awareness of the environment or the self. Sleep provides an additional valuable model of different and reversible states of consciousness, with the advantage of the possibility to record NCC-S of healthy participants. Indeed, there are clear EEG markers (Iber et al., 2007; Imperatori et al., 2021; Comsa et a., 2019) and fMRI activity patterns characterizing brain activity in wakefulness and during different sleep stages (Dang-Vu et al., 2010; Peigneux 2015; Song and Tagliazucchi 2021). Additional models of interest include anesthesia (Lewis et al., 2012; Barttfeld et al., 2015; Chennu et al., 2016; Zelmann et al., 2023) or complex seizures (Guo et al., 2016; Blumenfeld 2021).

All these results demonstrate a rich literature studying particular brain activity features as putative NCC-S or NCC-C. However, not much is known when it comes to comparing those given features in both NCC dimensions simultaneously; do the different NCC reflect identical or different neuronal processes relevant to both state and content of consciousness, or, alternatively, are they specific to only one of those dimensions?

In this work, we propose a two-dimensional space framework that allows the contrast of brain features in both NCC dimensions simultaneously, and to characterize different types of NCC according to where they fall in the two-dimensional space. We also provide two experimental examples: a comparison of states of consciousness

(disorders of consciousness or sleep) and of types of conscious content (auditory or visual).

Methods

Population

Patients

We included 443 patients (177 women; age = 47 ± 19) recorded between 2008 and 2019 in the neuro-intensive care at Pitié Salpetrière for an expert assessment of their consciousness. During this evaluation, we performed several exams (clinical assessment, MRI, EEG, ERP, PET) to determine more accurately the state of consciousness. The Ethical Committee of the Pitie-Salpetriere approved this research under the French label of ‘routine care research’ (Comité de Protection des Personnes n◦ 2013-A01385-40 Ile de France, Paris, France, under the code ‘Recherche en soins courants’).

Healthy subjects

Experiments were approved by the Ethical Committee of the Pitie Salpetriere Hospital, NeuroDoc protocol. We recorded 36 subjects (29 women; age = 25.3 ± 3.8 mean ± standard deviation) for the local-global paradigm, and 35 subjects (28 women; age = 24.9 ± 4.1 mean ± standard deviation) for the visual awareness paradigm. For the nap experiment, twenty-six participants (19 women; age = 24.3 ± 4.9 years mean ± standard deviation) were recruited to the study and gave written informed consent to procedures approved by the University of Cambridge Research Ethics Committee, in accordance with the Declaration of Helsinki.

Paradigms

Experiment 1: Local-global paradigm

The local-global paradigm, developed by Bekinschtein et al., is reported in Bekinschtein et al. (2009). This is an oddball paradigm based on the repetition of two sequences of tones: XXXXX or XXXXY. In a low-level (local regularity), XXXXX is the local standard and XXXXY is the local deviant. The contrast between these two sequences reveals the occurrence of the Mismatch Negativity (MMN). This response is in a short range and is also reproduced during the loss of consciousness associated with sleep, general anesthesia, or vegetative state. In a high level (global regularities), the repetition of the XXXXY or XXXXX is the standard condition and establishes the rule. The violation of this regularity by the other sequence: XXXXX or XXXXY respectively, is represented by the P3b waveform and requires conscious awareness and working memory. Local and global regularities are manipulated orthogonally 2*2: The first type of blocks consists of local standard-global standard (XXXXX) and local deviant-global deviant (XXXXY) sounds. The second type of blocks is made up of local deviant-global standard (XXXXY) and local standard-global deviant (XXXXX) sounds.

Experiment 2: Visual awareness paradigm

Near-threshold visual awareness was assessed using a visual backward masking paradigm modified from Del Cul et al. (Del Cul et al., 2007). In this paradigm, a para-foveal numerical target (‘2’, ‘3’, ‘7’ or ‘8’, height = 1.7 cm, width = 1.1 cm) was presented for 16 ms either to the right or to the left of a central fixation point (8° visual angle) on a 60 Hz frame-rate screen. The numerical target was followed after

a variable Stimulus Onset Asynchrony (SOA, to 16 ms at 83 ms) by a visual mask, consisting of letters surrounding the target, presented for 250 ms. 800 ms after the target presentation, participants were asked to perform a subjective task of visibility rating of the target through a binary ‘seen’ / ‘unseen’ answer. Answers were collected via key press with a pseudo-randomization of response hand order and switch of response hand in the middle of the task. The entire task consisted of the presentation of 400 trials (64 trials per SOA and 80 catch trials in which only a mask was presented, without a target).

Experiment 3: Nap

Participants arrived at the EEG lab either at 8:00 or at 13:00 and were accommodated in a bed and instructed that they have a 2-hours window during which they could fall asleep. They were informed that, while asleep, they might be presented with tones via the headphones and that, if they noticed them, they could ignore them and continue sleeping. The EEG signal was constantly monitored for markers of sleep. After having assessed stable non-rapid eye movement (NREM) sleep for at least three minutes, auditory stimulation including pure tones (500 Hz to 5302 Hz, 100ms, ISI = 500ms) was started. Tones were played with a slow fading-in to minimize the likelihood that participants would be awakened by the onset of the stimuli. Importantly, to minimize exposure to stimulation during arousals, whenever arousal occurred stimulation was promptly stopped. Stimulation would then be resumed only after a stable NREM sleep had been reassessed. For the goal of this study, we used sections of the recording during which no sounds were presented.

EEG processing data

Experiment 1: Local-global paradigm

The EEG data was recorded at a sampling frequency of 250 Hz with a 256-electrode geodesic sensor net (Electrical Geodesics Inc system) referenced to the vertex. Trials were band-pass filtered (0.5-45 Hz) and then segmented in epochs ranging from −200 ms to +1344 ms from the first sound onset. Electrodes with voltages exceeding 100μV in more than 50% of the epochs were removed. Moreover, voltage variance was computed across all correct electrodes. Electrodes with a voltage variance Z-score higher than four were removed. This process was repeated four times. Bad electrodes were interpolated using a spline method (Perrin et al., 1989). Epochs were labeled as bad and discarded when voltage exceeded 100μV in more than 10% of electrodes. Moreover, voltage variance was computed across all correct epochs, and epochs with a Z-score larger than 4 were removed. This process was also repeated four times. The remaining stimulus-locked epochs were averaged and digitally transformed to an average reference. A 200 ms baseline correction (before the fifth sound onset) was applied. Pre-processing was implemented using the MNE-Python package.

Experiment 2: Visual awareness paradigm

High-density scalp EEG was acquired using 256 electrodes Hydrocel Geodesic Sensor Net on a Net300 Amplifier (Electrical Geodesics Inc system) with a sampling frequency of 250 Hz during the behavioral task. Impedances were set to below 75 kΩ prior to the start of each recording. EEG was preprocessed using a fully automatic procedure (same preprocessing as for the local-global paradigm). The

only change is that the epochs are segmented between -300 ms to 800 ms according to the onset of the target.

In order to get rid of the confound of evoked responses to the mask, we proceeded to a mask subtraction procedure as in the Del Cul et al. study (Del Cul et al., 2007). We first realigned all epochs to the mask onset and computed the evoked response to the mask from the catch trials. We then subtracted this evoked response from all other trials. Finally, we realigned epochs on the target to obtain epochs stripped from the mask response (this procedure resulted in shortening the epochs which as a result went from -232 ms to 732 ms after target onset).

Experiment 3: Nap

The EEG signal was recorded with 128-channel sensors using a GES 300 Electrical Geodesic amplifier, at a sampling rate of 500 Hz (Electrical Geodesics Inc system/Philip Neuro). Conductive gel was applied to each electrode to ensure that the impedance between the scalp and electrodes was kept below 70 kΩ. The EEG recordings were then preprocessed using the same fully automatic procedure as for the local-global and visual awareness paradigms.

Two independent experienced sleep examiners blind to stimuli onset/offset times scored offline 30 s-long windows of EEG data according to established guidelines (Iber et al., 2007). The two scoring lists were subsequently compared and controversial epochs were inspected again and discussed until an agreement was reached. EEG and EOG signals were first re-referenced to mastoids and then EEG signals were bandpass filtered between 0.1 and 45Hz, EOG between 0.2 and 5Hz. EMG signals were obtained from local derivation and were high-pass filtered above

20 Hz. Then, based on the sleep scoring, periods of wakefulness (319.4 ± 33.5 sec) and NREM stage 2 sleep (369.8 ± 93.6 sec) when no auditory stimulation was presented were selected.

Two NCC dimensions according to the local-global paradigm and visual awareness paradigm

A set of previously proposed putative NCC (Engemann et al., 2018; Sitt et al., 2014) were computed in state of consciousness contrasts (NCC-S) and conscious content contrast (NCC-C). Importantly the algorithms and parameters used to compute the proposed markers were identical in both cases.

For the NCC-S, analyses were performed on the local-global EEG recording in the group of patients and a nap session in healthy participants. In the local-global dataset, analyses were carried out from -100 ms before the onset of the first sound to the onset of the fifth sound (+600 ms). All trials are selected independently of standard or deviant status. This was combined with the nap EEG data which was split into epochs of 800 ms, separately for the periods of NREM stage 2 sleep or wakefulness. The epoching was done using a random jitter, between two epochs, from 550 ms to 850 ms.

In this range, three types of markers were computed: 1) Markers of connectivity: wSMI in the theta band. 2) Markers of complexity: Kolmogorov-Chaitin complexity and permutation entropy. 3) Markers of frequency power: alpha power, beta power, delta power, gamma power, theta power. The result is expressed with AUC corresponding to the estimation of the classifier's ability to discriminate between MCS and VS/UWS patients or between wakefulness and N2 sleep.

For the NCC-C, the local-global EEG recording was used in healthy subjects from +600ms (onset of the fifth sound) and +1300ms. The EEG was also recorded during the visual awareness paradigm in the healthy subject, the window of interest is between the presentation of the numerical target (0ms) and +700ms. The same markers used as NCC-S were calculated but contrasted between deviant/standard trials or seen/not-seen trials. The result is expressed with AUC corresponding to the estimation of the classifier's ability to discriminate GD and GS trials, LD and LS trials, or seen/not-seen trials.

Statistics

AUC

The area under the curve (AUC) is calculated from the receiver operating characteristic (ROC) curve. The ROC curve is a graph representing the performance of a classification model for all classification thresholds. It is plotted from the rate of true positives (sensitivity) versus the rate of false positives (1-specificity). It is then possible to calculate the area under this curve, or AUC, using a sorting algorithm. The AUC provides an aggregate measure of performance for all possible classification thresholds. The AUC can be interpreted as a measure of the probability that the EEG marker used will correctly classify trials or conditions (here, UWS/MCS patients, wake/N2 sleep in healthy participants, GD/GS, LD/LS; or seen/unseen trials). An AUC value close to 1 shows that the marker is higher in the A condition than in the B condition, close to 0.5 the classifier is at random, and an AUC value close to 0 shows that the marker is higher in the B condition than the A condition. For the paired conditions (seen/unseen; GD/GS; LD/LS; wake/N2 sleep), the distributions of the markers per epoch were z-scored, and the trimmed means were

calculated (excluding the bottom and top 10 % of the distributions). This results in one value per subject per condition per marker. The AUC values were calculated on these group-level distributions. For the UWS/MCS recordings, the same analysis was done with the exception of z-scoring. We report significant AUC for the content or the state if the AUC values of the two distributions are significantly different with a Wilcoxon two-sided test, Bonferroni corrected - for the paired conditions and a Mann-Whitney U test, Bonferroni corrected - for the unpaired condition (UWS/MCS).

Computation of markers

Normalized power spectral analysis

Spectral analysis is a well-established method for the analysis of EEG signals. We estimated power in five frequency bands (delta to gamma: Delta (δ: 1-4 Hz), Theta (θ: 4-8 Hz), Alpha (α: 8-13 Hz), Beta (β: 13-30 Hz) and Gamma (γ: 30-45 Hz)). Mathematically, the power spectral density is estimated by the Welsh method (Welch, 1967). The power in a given band is calculated as the integral of the spectral power density then it is linearized using a logarithmic scale. The normalized power is calculated by dividing the power in each band by the total energy in the trial. It is expressed in dB and therefore represents a percentage of power. The abbreviations used in the text for the normalized power bands are the following: Delta normalized |δ|, Theta normalized |θ|, Alpha normalized |α|, Beta normalized |β|, Gamma normalized |γ|.

Markers of complexity

Permutation entropy (PE) was developed by Bandt & Pompe (Bandt & Pompe, 2002). The basic principle of this method is the transformation of the time signal into

a sequence of symbols before estimating entropy. The complete description is given in Sitt, Brain, 2014 (Sitt et al., 2014) The transformation is made by considering consecutive sub-vectors of the signal of size n (n=3 here) and a parameter defining a specific frequency band. After the symbolic transform, the probability of each symbol is estimated, and PE is computed by applying Shannon's entropy formula to the probability distribution of the symbols.

The complexity of Kolmogorov Chaitin (KS) is represented by the size of the smallest computer program that can be made to define this signal. The lower limit is therefore estimated by applying lossless compression, that is to say, a compression that restores after decompression a series of bits strictly identical to the original. The degree of compression is then compared to the basic signal. Here we use an open-source compressor: gzip. It uses a compression algorithm, a method called Deflate including the LZ77 algorithm and Huffman coding.

The first is based on dictionary compression by transforming the sequence into 32 symbols, then we replace the recurring sequences with the position and the length of the occurrences in a sliding window. The second is based on the construction of a tree where we assign to each redundant sequence - a weight. Thus, after having calculated the number of occurrences of a sequence, the more redundant the sequence the more a small number of bits is allocated to code it. Compression by gzip is therefore based on signal redundancy. We then compare the size of the compression compared to the initial file. The more compressed the file, the less information it contains.

Markers of connectivity

The weighted symbolic mutual information (wSMI) can be used to evaluate long-distance connectivity, details of the calculation are developed in King (King et al., 2013). The wSMI is a measure based on the prediction of the theory of the global workspace and of experiments concerning the conscious perception of subliminal stimuli. Indeed, several studies (Dehaene et al., 2003) have shown a late use of the frontoparietal network and above all an increase in the sharing of information between brain areas. The EEG signal is transformed into a sequence of six symbolic figures then the permutation entropy (PE) is calculated: we then take each pair of electrodes and observe the conjunction of symbolic elements. Mutual information measures the quantity of information distributed on average by a realization of X over the probabilities of realization of Y. The SMI is weighted to ignore conjunctions of identical or opposite symbols that may come from a common source of artifacts. The connectivity measurement is obtained by taking the median value of all pairs of electrodes.

Results

The 2D-representation: state versus content

We have shown the difficulty of studying the state and content of consciousness under the same dimension. For the framework we represent the performance of a given NCC marker using the area under the receiver operating characteristic curve (AUC) contrasting two states of consciousness conditions (x-axis) or two content of consciousness conditions (y-axis). The AUC represents the probability of the

proposed NCC to discriminate between two conditions, in a value between 0 and 1 (1 means correct classification of all subjects, 0.5 is considered chance level).

First, we use the contrast between VS/UWS patients and MCS patients, the vegetative state as a state of wakefulness without awareness and the minimally conscious state as an awake state with minimal or inconsistent awareness of self or the environment. Second, we used another popular contrast, the comparison of NCC-S during wakefulness versus stage 2 (N2) of non-rapid eye movement (NREM) sleep in healthy participants.

In our examples, conscious content (on the y-axis) is represented by the same markers used in the x-axis but in this case contrasting a perceptual task between a conscious condition and an unconscious condition. We also use the AUC of each marker to differentiate between conscious and unconscious conditions. We used two examples of conscious content tasks in healthy participants: 1) auditory local-global paradigm using a complex auditory oddball paradigm and 2) visual awareness paradigm using a visual backward masking paradigm (see methods).

The proposed axes divide the plane into four quadrants, subdivided into 9 zones. The correspondence of each marker to a given quadrant determines how the marker behaves in terms of state and content (Figure 1). Top right (AUC-x > 0.5 and AUC-y > 0.5) and bottom left (AUC-x < 0.5 and AUC-y < 0.5) quadrants in light violet correspond to markers that behave in unity in the state and content dimensions (increase in conscious state and conscious content, or decrease in both dimensions). In contrast, the top left (AUC-x < 0.5 and AUC-y > 0.5) and bottom right (AUC-x > 0.5 and AUC-y < 0.5) quadrants in dark violet correspond to markers that have opposite behaviors in both dimensions (increase in conscious state and

decrease conscious content, or vice-versa). In addition, two blue / red zones around the x / y axis correspond to either an increase or decrease of the markers that are only valid for state (x, blue) or content (y, red) and the white area around 0.5 correspond to markers with no state- or content-specific information. The white zone in the middle of the plane represents markers unrelated to either state of content.

This framework is generalizable across functional modalities and markers. Here we use EEG recordings that have a high temporal resolution and can capture fast neural changes in response to the aforementioned task paradigms. But this framework can be extended to other neuroimaging modalities that allow distinction of state and content of consciousness (e.g. fast functional magnetic resonance, MEG, intracranial recordings, fNIRS, calcium imaging). The markers used in this study belong to a few conceptual families in neural dynamics (spectral, information theory and connectivity) and are defined in Sitt & King et al. (2014) and Engemann & Raimondo et al. (2018) (also see Methods, Computation of markers). These markers have been shown to have discriminatory power across the DoC (Sitt & King et al., 2014; Engemann & Raimondo et al., 2018) and sleep spectra (Strauss et al., 2022, Turker & Musat & Chabani et al., 2023).

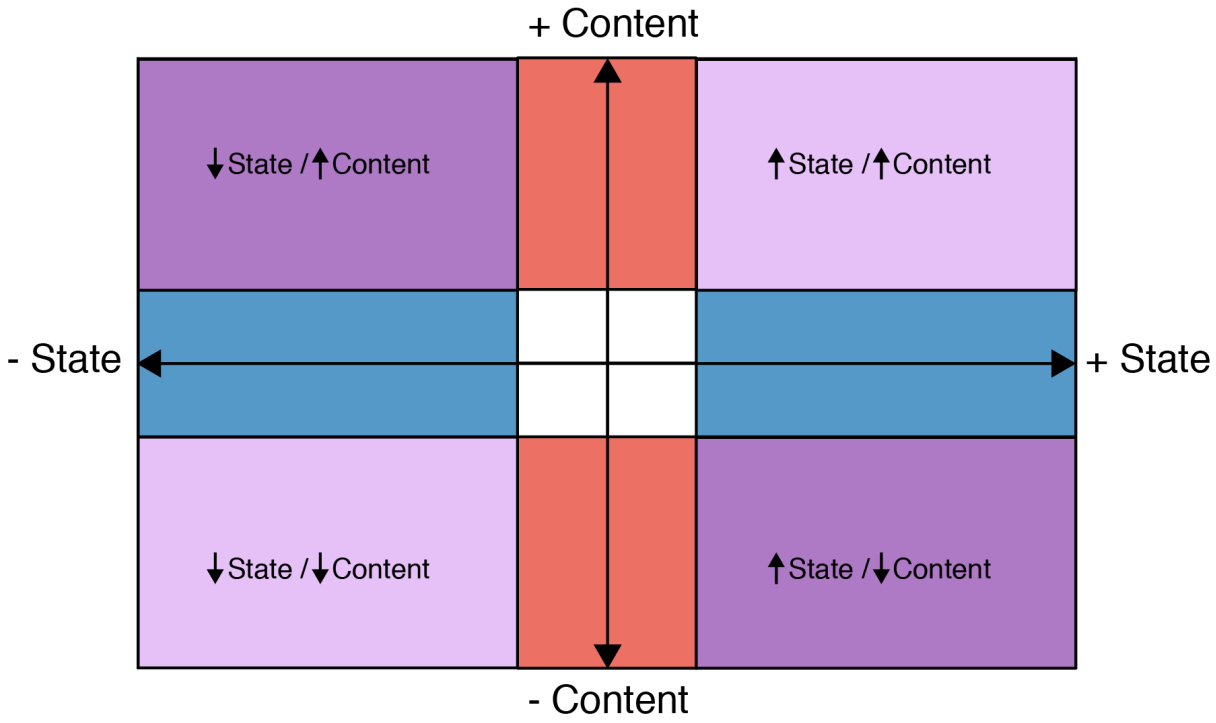

Figure 1: A 2D representation of state of consciousness and conscious content. The decomposition of the space forms four quadrants. The light purple quadrants correspond to the quadrants in which the content markers decrease when the level of consciousness decreases and vice versa. Dark purple quadrants correspond to an increase of content markers when the level of consciousness decreases (or vice-versa). The blue band is the pure NCC-state, the red band is the pure NCC-content and the white area is not specific to either NCC-state or NCC-content.

Example 1: Auditory local-global paradigm and disorders of consciousness

State: We recorded high-density EEG during the active 'local-global' task (see methods) in 388 disorders of consciousness patients (behavioral exam according to CRS-R: 191 MCS and 197 VS/UWS) referred to our team at the Pitié-Salpêtrière University Hospital in Paris for diagnostic and prognostic evaluations of

consciousness. The same paradigm was used to obtain EEG recordings in 36 healthy participants.

Content: The local-global task (see methods) is an oddball auditory paradigm that has two hierarchical levels of regularities: a "Local" regularity that triggers early responses that are preserved in conscious and unconscious states, and a "Global" regularity which triggers late evoked responses that are only present in awake, conscious, and attentive subjects (Bekinschtein et al., 2009; J. R. King et al., 2013; Strauss et al., 2015; Wacongne et al., 2011, Chennu et al., 2013). The neural responses to the violation of each of these regularities can be quantified from two complementary contrasts, the local contrast (local deviant (LD) trials versus local standard (LS) trials) and the global contrast (global deviant (GD) trials versus global standard (GS) trials). Here we focus on the global contrast as it indicates some level of conscious content processing. In addition, this paradigm allows the computation of different putative markers from segments of "pseudo-resting-state" (during the stimulation (Engemann et al., 2018)) to contrast their power to index the different states of consciousness in patients regardless of the stimulus content (Sitt et al., 2014).

In this example, we represent different EEG markers in the proposed two-dimensional space in order to differentiate their behavior according to the state of consciousness or the conscious content (Figure 2). In the x-axis, representing level, we use the “pseudo resting state” (see methods) of patients' data and we order the markers according to the AUC on the VS/UWS versus MCS contrast. For the y-axis, representing content, we used the global-local paradigm in healthy

participants' data and we sorted the markers according to the AUC on the GD versus GS conditions (Figure 2).

At first glance, one can observe that the markers are arranged in all four quadrants. Surprisingly, several of the markers (|α|, wSMI, PE, see the Methods for the marker abbreviations) are located in the lower right quadrant, meaning that these markers increase with the state of consciousness but decrease with conscious content. Conversely, |δ| is on the upper left quadrant, indicating increasing values for conscious content but decreasing for the state of consciousness. Finally, other markers like |β|, |γ|, or KS were only significant for conscious content but not for state. Finally, |θ| was only significant for the conscious state but not for content, reflecting increasing values with the state of consciousness (minimally conscious > vegetative states).

Notably, a sharp difference in the AUC of the EEG markers can be observed when Local or Global contrasts are used for the content dimension (Figure 2. B, and Supplementary Figure 1). The performance of the NCC to distinguish LD versus LS is systematically lower compared to GD versus GS (p-value 0.016 of a paired Wilcoxon signed-rank test). All but one (|θ|) of the NCC shows a better discriminative performance for the Global effect in contrast to the Local effect.

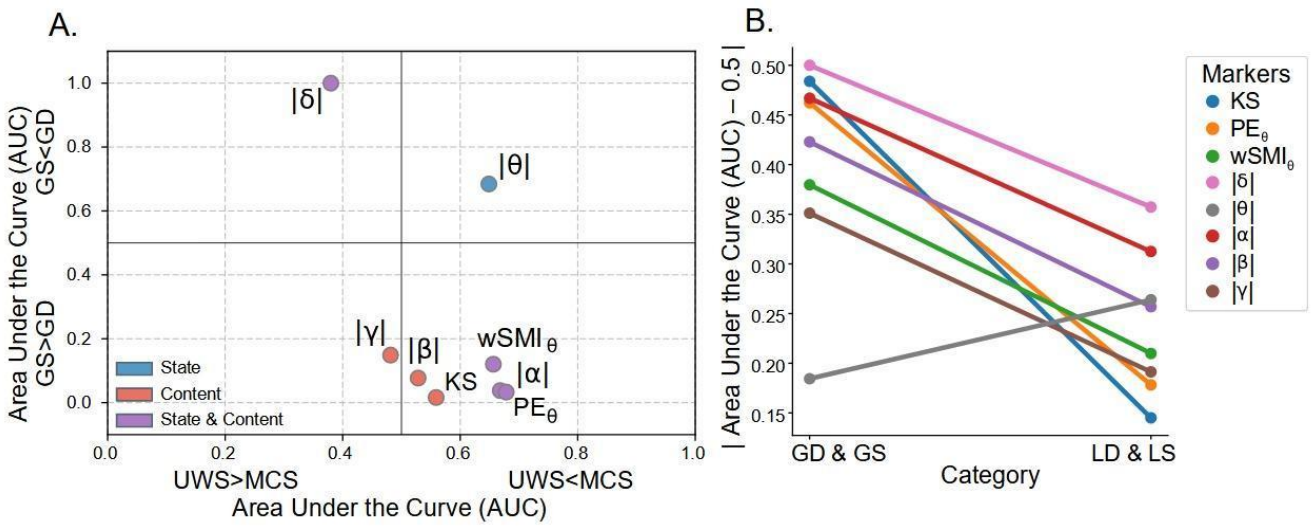

Figure 2: A. Example #1, distribution of EEG markers in the state and content dimensions for the auditory modality and disorders of consciousness patients.

The coordinate of each point in the x-axis represents the ability of the marker to discriminate between VS/UWS and MCS patients. The coordinate at the same point in the y-axis represents the ability of the marker to discriminate between the global deviant and the global standard trials in the local-global paradigm in healthy participants. Note that the crossing of the x-axis and y-axis is centered at 0.5, which corresponds to discrimination at the level of chance. Points are colored according to their statistical significance in either the content dimension, the state dimension or both. **B**: The performance of EEG markers to discriminate GD to GS is higher than the power of EEG markers to discriminate LD to LS. The detection of the global deviant is a marker of conscious content whereas the local deviant is an automatic response to the novelty. In the figure, 0.5 is subtracted from the values of the AUC. See the Methods for marker abbreviations.

Example 2: Visual awareness paradigm and nap in healthy participants

State: In this second example, for the x-axis, we use 26 EEG recordings in healthy participants during a nap opportunity of two hours and we order the markers according to the AUC discrimination on wakefulness versus N2 sleep.

Content: for the Y-axis we used high-density EEG recordings in 35 healthy participants during a visual, backward masking, awareness paradigm (Del Cul et al., 2007). This visual awareness paradigm is designed to suppress visual perception by presenting a visual stimulus ('mask') immediately after another visual stimulus ('target'). This manipulation causes a failure of the first stimulus perception. In this example, the values for each marker on the y-axis are determined by the AUC when contrasting seen versus unseen trials (Figure 3).

Similar to the results obtained in experiment 1, most of the markers are on the lower right half of the graph (|α|, |β|, |γ|, KS, wSMI, PE) but contrary to the first experiment, none of the markers are content-only. Interestingly, wSMI, KS, PE, and |α| are significant only for state, whereas |β| and |γ| are significant for both state and content. The two last markers |δ|, |θ| are in the top left quadrant and significant for both state and content which means that they increase for content while they decrease with the state of consciousness.

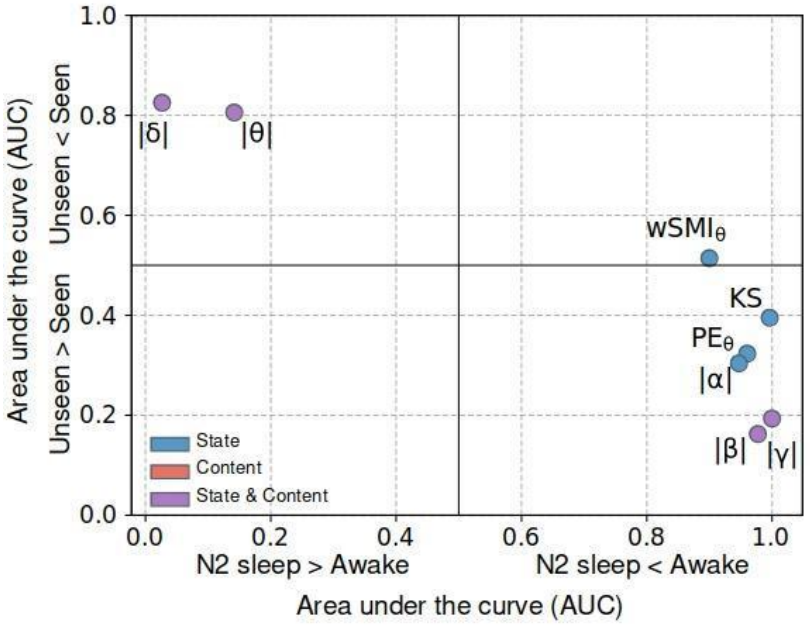

Figure 3: Example #2, Behavior of EEG markers in the state and content dimensions for the visual awareness dataset and healthy participants nap. The coordinate of each point in the x-axis represents the ability of the marker to discriminate between wakefulness and N2 sleep. The coordinate in the Y-axis of the same point represents the ability of the marker to discriminate between seen and not-seen targets during the visual awareness paradigm. See the Methods for the marker abbreviations.

Discussion

In this work we propose a framework that permits the direct comparison of neural correlates of conscious state and conscious content in the same space. With two implementation examples we show that neural correlates depict different properties in discriminating these dimensions of consciousness.

While several studies have attempted to study content and state separately, a theoretical development proposes a three-dimensional axis with an x-axis

corresponding to subjective conscious content (as reported by the subject), the y-axis to the objective state of consciousness (defined by behavior and body signals), and the z-axis to a subjective state of consciousness (as reported by the subject) (Bachmann, 2012). In the examples presented here we used NCCs of objective state of consciousness in the Y axis. However, the proposed framework is also compatible when subjective state NCCs are considered. Bayne and colleagues on the other hand, propose a multidimensional graph like a radar chart with different axes (Bayne et al., 2016): content-related (e.g., content gating and content range) and functional dimensions (e.g., relating to attentional control, memory consolidation, verbal report, reasoning, action selection, etc.). The problem with this representation is that it is difficult to standardize and, hence, less applicable. Interestingly, Sergent and colleagues (Sergent et al., 2017) created a unique EEG protocol allowing to explore 8 axes (own name recognition, temporal attention, spatial attention, detection of spatial incongruence motor planning, and modulations of these effects by the global context) but the construction of such a paradigm is complex.

For Chalmers, studying content and conscious state at the same time is difficult in experimental conditions (Chalmers, 1997), with most studies contrasting variable content in a given state of consciousness or studying brain differences in different states. Thus, the challenge in this two-dimensional representation of NCC is to find a minimal relevant contrast. In these two examples, we contrast both, conscious state and conscious content, but independently. The state was studied by contrasting either wakefulness and sleep or VS/UWS patients and MCS patients classified in the clinic, since the MCS state is considered an altered state of consciousness and the VS/UWS state as a state of wakefulness without awareness. However, we have to note here that the VS/UWS versus MCS contrast is less dichotomous than it seems

due to the possibility that some VS/UWS patients are in a covert conscious condition (as called cognitive motor dissociation - CMD) (Owen et al., 2006; Schiff, 2015) as well as the heterogeneity within the two clinical categories (Naccache 2018; Hermann & Sangare et al., 2021).

We also studied the condition by contrasting healthy subjects in non-REM N2 sleep and in the awake state. The interest of such an approach is to show that the study of the different global states of consciousness also works for healthy participants.

The framework is flexible and can be extended to, for example, higher level states of consciousness such as MCS+ versus MCS- but also to choose contrasts in other circumstances: rapid eye movement (REM) sleep, lucid dreams or anesthesia in healthy participants.

The conscious content was studied in two modalities: auditory and visual. There is a high distance in the contrast of the conscious content between the sensory modalities, but also due to the type of perceptual processing (masking, threshold vision, detection of novelty), the challenge is to find a sufficiently salient contrast between the conscious and unconscious condition to capture, unambiguously, the cognitive/perceptual differences to obtain a robust neural characterization.

The first example, the auditory local-global paradigm is particularly powerful because it allows for a dual analysis, first, the study of the early, automatic response to novelty (Figure 2 B and Supplementary Figure 1), and second, the late and conscious response (Figure 2). The first analysis of this experience is therefore a kind of control, since previous studies demonstrated that the brain processing of this rule does not require conscious awareness. In this example, we confirm with the

local-deviant / local-standard (LD/LS) contrast that the putative NCC (EEG markers) are less able to discriminate between the two conditions compared to the global-deviant / global-standard (GD/GS) contrast.

The second example, wake-sleep and visual conscious access, uses the proposed representation with a different task such as a visual perception protocol as well as other states of consciousness such as NREM sleep. Comparison between the two examples highlights and challenges the fact that the different EEG markers evolve in the same direction according to the level of consciousness and the conscious content.

Our original hypothesis was that most markers would be located in the light purple quadrants (top-right and bottom left) of the graphical representation (see Figure 1), i.e. markers that increase with the state of consciousness and that also increase with the conscious content. In fact, most of the NCC lie in the quadrants of the inverse relationship between state and content suggesting that they might play different roles in the state and content contrast. This result stresses the relevance of the proposed 2D framework to characterize simultaneously the behavior of NCC in both the state and content dimensions.

Although the analyses of the exact location of each NCC lie beyond the original objectives of this work (because this location depends on the used cognitive protocol or the exact methodological recipe to compute them) we will anyhow try to briefly interpret them. The results in spectral power are consistent with some previous work: while delta decreases with higher states of consciousness theta and alpha both increase and higher frequencies are less informative (Sitt and King et al. 2014). In terms of conscious content, we found that delta and theta were higher in seen

conditions, which may reflect the slow late potentials associated with conscious access, a process uniquely underlying awareness. Contrary to some results in the literature we also found a reduction of gamma power, this is likely due to the more careful computation we used (20-40 Hz, average across all electrodes and normalized to the full spectrum power), as supported by Dwarakanath and colleagues (Dwarakanath et al., 2023), who investigate the changes in conscious content in the prefrontal cortex using a binocular rivalry paradigm and show that there is a suppression of 20-40 Hz activity concurrent with 1-9 Hz transients, both of which follow the exogenous stimulus changes of physical stimulus alternations. Importantly, these high-frequency suppressions and 1-9 Hz transients, precede the endogenous binocular rivalry perceptual transitions.

The same is true for markers of complexity and functional connectivity that decrease in the post-perceptual period with conscious content. This could be explained by a "gating" mechanism, where the conscious perceptual input would close, creating a refractory period, which is reflected in a decrease of these markers in post-perceptual time. The reduction in complexity with conscious content is also compatible with the proposal of higher stability of neuronal activity during conscious access (Schurger et al., 2015). Conversely, the NCC-S markers have a more intuitive interpretation that is aligned with existing literature. The NCC-S markers analysis in the second example (Figure 3) is mostly consistent with well-established knowledge of the relative spectral characteristics of wakefulness versus various sleep stages (Iber et al., 2007; Imperatori et al., 2021). In N2 sleep, we observe an increase in the relative delta and theta powers, as well as a decrease in alpha, beta, and gamma bands, which is aligned with previous reports (Imperatori et al., 2021, where all band comparisons are reported to be significant except for theta).

Furthermore, we observe an increase in wSMI for the theta band in N2 sleep, which is present, but not strong enough, in Imperatori et al., 2021.

Reflecting on Figure 3, we can therefore think that there is a temporal constraint on the functional cognitive architecture theorized under the name of a cognitive cycle (Madl et al., 2011). According to its authors, awareness would consist of cascading cycles of recurrent cerebral events. Each cognitive cycle would then detect the current situation and interpret it according to a given context. According to Franklin and colleagues (Franklin et al., 2005), "conscious events occur as a sequence of discrete, coherent episodes separated by quite short periods of no conscious content" similar to the frames of a movie, these frames of consciousness would be discrete but the conscious experience would seem continuous. A complementary framework is proposed by Herzog et al. (2016) where the authors argue for a rendering of the unconscious content in discrete conscious moments. They propose a two-stage model which is different from ‘snapshot’ theories. Visual information is processed unconsciously with a high temporal resolution followed by a discrete conscious percept (the outputs of unconscious processing) at a slower rate than the visual sampling (Herzog et al., 2016). This rate of conscious percepts is not fixed but depends on the unconscious processing reaching an attractor state (Herzog et al., 2016).

The two examples presented here should only be considered use cases and we postulate that the proposed space characterizing NCC should be compatible with types of contrasts represented in the Y-axis (e.g. crowding protocols, subliminal images, binocular rivalry, non-report paradigms, etc.) or in the X-axis (e.g. anesthesia, epileptic seizures, developmental stages, etc.). In a similar vein, the

NCC that we used to populate the 2D space are examples of EEG-based NCC used in the literature, our proposed framework permits to include any NCC (and in any neuroimaging modality) as long as it can be computed in state and content assessments.

We would like to emphasize that although we map the space of these content and level correlates, we do not imply that only empirical correlates of consciousness (and not their underlying mechanisms) can be studied. Ideas coming from information theory such as the information decomposition approach (Mediano et al., 2022; Vinck et al., 2023) and biophysical models (Luppi et al., 2023) try to capture the neural signatures that are potential echoes (and not correlates) of the neural implementation of the processing of a content or the underlying dynamics that maintain a specific state. The framework that we propose, can in turn be used as one form of evaluation of these models. For example, summary metrics of a biophysical model, or neural signatures that can be interpreted in terms of information and not simple communication or shared oscillatory activity, can be put into the two-dimensional space and depending on whether they underlie processes of states of consciousness or process of the perception of specific contents, they will be expected in a certain quadrant.

Conclusion

We show that it is possible to represent in a two-dimensional space representing NCC performance discriminating content and state of consciousness, and also its commonalities. The proposed space is valid in different perceptual modalities with diverse contrasts. The values of this representation are both theoretical and experimental because it allows to disentangle content and state of consciousness

signatures by studying multiple contrasts in the same framework, constituting an important tool to better interpret the true neuronal mechanisms underlying consciousness and cognition in different states and for different contents.

Bibliography

Bachmann, T. (2012). How to Begin to Overcome the Ambiguity Present in Differentiation between Contents and Levels of Consciousness? *Frontiers in Psychology*, *3*. https://doi.org/10.3389/fpsyg.2012.00082

Bandt, C., & Pompe, B. (2002). Permutation Entropy: A Natural Complexity Measure for Time Series. *Physical Review Letters*, *88*(17), 1–4. https://doi.org/10.1103/PhysRevLett.88.174102

Barttfeld, P., Uhrig, L., Sitt, J. D., Sigman, M., Jarraya, B., & Dehaene, S. (2015). Signature of consciousness in the dynamics of resting-state brain activity. Proceedings of the National Academy of Sciences of the United States of America, 112(3), 887–892. https://doi.org/10.1073/PNAS.1418031112

Bayne, T., Hohwy, J., & Owen, A. M. (2016). Are There Levels of Consciousness? *Trends in Cognitive Sciences*, *20*(6), 405–413. https://doi.org/10.1016/j.tics.2016.03.009

Bekinschtein, T. A., Dehaene, S., Rohaut, B., Tadel, F., Cohen, L., & Naccache, L. (2009). Neural signature of the conscious processing of auditory regularities. *Proceedings of the National Academy of Sciences of the United States of America*, *106*(5), 1672–1677. https://doi.org/10.1073/pnas.0809667106

Blumenfeld, H. (2021). Arousal and Consciousness in Focal Seizures. Epilepsy Currents, 21(5), 353–359. https://doi.org/10.1177/15357597211029507

Boly, M., Seth, A. K., Wilke, M., Ingmundson, P., Baars, B., Laureys, S., Edelman, D. B., & Tsuchiya, N. (2013). Consciousness in humans and non-human animals: Recent advances and future directions. *Frontiers in Psychology*, *4*, 625. https://doi.org/10.3389/fpsyg.2013.00625

Casarotto, S., Comanducci, A., Rosanova, M., Sarasso, S., Fecchio, M., Napolitani, M., Pigorini, A., G Casali, A., Trimarchi, P. D., Boly, M., Gosseries, O., Bodart, O., Curto, F., Landi, C., Mariotti, M., Devalle, G., Laureys, S., Tononi, G., & Massimini, M. (2016). Stratification of unresponsive patients by an independently validated index of brain complexity. *Annals of Neurology*, *80*(5), 718–729. https://doi.org/10.1002/ana.24779

Chalmers, D. J. (1997). Moving forward on the problem of consciousness. *Journal of Consciousness Studies*, *4*(1), 3–46.

Chennu, S., Noreika, V., Gueorguiev, D., Blenkmann, A., Kochen, S., Ibáñez, A., Owen, A. M., & Bekinschtein, T. A. (2013). Expectation and Attention in Hierarchical Auditory Prediction. *Journal of Neuroscience*, *33*(27), 11194–11205. https://doi.org/10.1523/JNEUROSCI.0114-13.2013

Chennu, S., Finoia, P., Kamau, E., Allanson, J., Williams, G. B., Monti, M. M., Noreika, V., Arnatkeviciute, A., Canales-Johnson, A., Olivares, F., Cabezas-Soto, D., Menon, D. K., Pickard, J. D., Owen, A. M., & Bekinschtein, T. A. (2014). Spectral Signatures of Reorganised Brain Networks in Disorders of Consciousness. *PLOS Computational Biology*, *10*(10), e1003887. https://doi.org/10.1371/JOURNAL.PCBI.1003887

Chennu, S., O'Connor, S., Adapa, R., Menon, D. K., & Bekinschtein, T. A. (2016). Brain Connectivity Dissociates Responsiveness from Drug Exposure during

Propofol-Induced Transitions of Consciousness. PLOS Computational Biology, 12(1), e1004669. https://doi.org/10.1371/JOURNAL.PCBI.1004669

Comsa, I. M., Bekinschtein, T. A., & Chennu, S. (2019). Transient Topographical Dynamics of the Electroencephalogram Predict Brain Connectivity and Behavioural Responsiveness During Drowsiness. Brain Topography, 32(2), 315–331. https://doi.org/10.1007/s10548-018-0689-9

Crick, F., & Koch, C. (1990). Toward a Neurobiological Theory of Consciousness. *Seminars in the Neurosciences*, *2*, 263–275.

Dang-Vu, T.T., Schabus, M., Desseilles, M., Sterpenich, V., Bonjean, M., Maquet, P. (2010) 'Functional neuroimaging insights into the physiology of human sleep', Sleep, 33(12), pp. 1589–1603. https://doi.org/10.1093/sleep/33.12.1589

Dehaene, S., Sergent, C., & Changeux, J.-P. (2003). A neuronal network model linking subjective reports and objective physiological data during conscious perception. *Proceedings of the National Academy of Sciences of the United States of America*, *100*(14), 8520–8525. https://doi.org/10.1073/pnas.1332574100

Dehaene, S., & Changeux, J.-P. (2011). Experimental and theoretical approaches to conscious processing. *Neuron*, *70*(2), 200–227. https://doi.org/10.1016/j.neuron.2011.03.018

Del Cul, A., Baillet, S., & Dehaene, S. (2007). Brain dynamics underlying the nonlinear threshold for access to consciousness. *PLoS Biology*, *5*(10), e260. https://doi.org/10.1371/journal.pbio.0050260

Demertzi, A., Gómez, F., Crone, J. S., Vanhaudenhuyse, A., Tshibanda, L., Noirhomme, Q., Thonnard, M., Charland-Verville, V., Kirsch, M., Laureys, S., & Soddu, A. (2014). Multiple fMRI system-level baseline connectivity is

disrupted in patients with consciousness alterations. *Cortex; a Journal Devoted to the Study of the Nervous System and Behavior*, *52*, 35–46. https://doi.org/10.1016/j.cortex.2013.11.005

Demertzi, A., Antonopoulos, G., Heine, L., Voss, H. U., Crone, J. S., de Los Angeles, C., Bahri, M. A., Di Perri, C., Vanhaudenhuyse, A., Charland-Verville, V., Kronbichler, M., Trinka, E., Phillips, C., Gomez, F., Tshibanda, L., Soddu, A., Schiff, N. D., Whitfield-Gabrieli, S., & Laureys, S. (2015). Intrinsic functional connectivity differentiates minimally conscious from unresponsive patients. *Brain: A Journal of Neurology*, *138*(Pt 9), 2619–2631. https://doi.org/10.1093/brain/awv169

Demertzi, A., Tagliazucchi, E., Dehaene, S., Deco, G., Barttfeld, P., Raimondo, F., Martial, C., Fernández-Espejo, D., Rohaut, B., Voss, H. U., Schiff, N. D., Owen, A. M., Laureys, S., Naccache, L., & Sitt, J. D. (2019). Human consciousness is supported by dynamic complex patterns of brain signal coordination. Science Advances, 5(2). https://doi.org/10.1126/sciadv.aat7603

Di Perri, C., Bahri, M. A., Amico, E., Thibaut, A., Heine, L., Antonopoulos, G., Charland-Verville, V., Wannez, S., Gomez, F., Hustinx, R., Tshibanda, L., Demertzi, A., Soddu, A., & Laureys, S. (2016). Neural correlates of consciousness in patients who have emerged from a minimally conscious state: A cross-sectional multimodal imaging study. *The Lancet. Neurology*, *15*(8), 830–842. https://doi.org/10.1016/S1474-4422(16)00111-3

Engemann, D. A., Raimondo, F., King, J.-R., Rohaut, B., Louppe, G., Faugeras, F., Annen, J., Cassol, H., Gosseries, O., Fernandez-Slezak, D., Laureys, S., Naccache, L., Dehaene, S., & Sitt, J. D. (2018). Robust EEG-based cross-site

and cross-protocol classification of states of consciousness. *Brain: A Journal of Neurology*, *141*(11), 3179–3192. https://doi.org/10.1093/brain/awy251

Giacino, J. T., Ashwal, S., Childs, N., Cranford, R., Jennett, B., Katz, D. I., Kelly, J. P., Rosenberg, J. H., Whyte, J., Zafonte, R. D., & Zasler, N. D. (2002). The minimally conscious state: Definition and diagnostic criteria. *Neurology*, *58*(3), 349–353. https://doi.org/10.1212/wnl.58.3.349

Goupil, L., & Bekinschtein, T. (2012). Cognitive processing during the transition to sleep. *Archives italiennes de biologie*, *150*(2/3), 140-154.

Guo, J. N., Kim, R., Chen, Y., Negishi, M., Jhun, S., Weiss, S., Ryu, J. H., Bai, X., Xiao, W., Feeney, E., Rodriguez-Fernandez, J., Mistry, H., Crunelli, V., Crowley, M. J., Mayes, L. C., Constable, R. T., & Blumenfeld, H. (2016). Mechanism of impaired consciousness in absence seizures: a cross-sectional study. The Lancet. Neurology, 15(13), 1336. https://doi.org/10.1016/S1474-4422(16)30295-2

Hermann, B., Stender, J., Habert, M. O., Kas, A., Denis-Valente, M., Raimondo, F., Pérez, P., Rohaut, B., Sitt, J. D., & Naccache, L. (2021). Multimodal FDG-PET and EEG assessment improves diagnosis and prognostication of disorders of consciousness. *NeuroImage: Clinical*, *30*. https://doi.org/10.1016/j.nicl.2021.102601

Hermann, B., Sangaré, A., Munoz-Musat, E., Salah, A. ben, Perez, P., Valente, M., Faugeras, F., Axelrod, V., Demeret, S., Marois, C., Pyatigorskaya, N., Habert, M.-O., Kas, A., Sitt, J. D., Rohaut, B., & Naccache, L. (2021). Importance, limits and caveats of the use of “disorders of consciousness” to theorize consciousness. *Neuroscience of Consciousness*, *2021*(2), 1–13. https://doi.org/10.1093/NC/NIAB048

Herzog, M. H., Kammer, T., & Scharnowski, F. (2016). Time Slices: What Is the Duration of a Percept? *PLOS Biology*, *14*(4), e1002433. https://doi.org/10.1371/JOURNAL.PBIO.1002433

Iber, C., Ancoli-Israel, S. & A, C. (2007). The AASM manual for the scoring of sleep and associated events: Rules, terminology and technical specifications. American Academy of Sleep Medicine.

Imperatori, Laura Sophie and Cataldi, J., Betta, M., Ricciardi, E., Ince, R. A.A., Siclari, F., Bernardi, G. (2021). Cross-participant prediction of vigilance stages through the combined use of wPLI and wSMI EEG functional connectivity metrics, Sleep, 44(5), pp. 1–14. https://doi.org/10.1093/sleep/zsaa247

Jennett, B., & Plum, F. (1972). Persistent vegetative state after brain damage. *RN*, *35*(10), ICU1-4.

Kalmar, K., & Giacino, J. T. (2005). The JFK Coma Recovery Scale—Revised. *Neuropsychological Rehabilitation*, *15*(3–4), 454–460. https://doi.org/10.1080/09602010443000425

Kim, C.-Y., Blake, R. (2005). Psychophysical magic: Rendering the visible “invisible.” *Trends in Cognitive Sciences*, *9*(8), 381–388. https://doi.org/10.1016/j.tics.2005.06.012

King, J. R., Faugeras, F., Gramfort, A., Schurger, A., El Karoui, I., Sitt, J. D., Rohaut, B., Wacongne, C., Labyt, E., Bekinschtein, T., Cohen, L., Naccache, L., & Dehaene, S. (2013). Single-trial decoding of auditory novelty responses facilitates the detection of residual consciousness. *NeuroImage*, *83C*(null), 726–738. https://doi.org/10.1016/j.neuroimage.2013.07.013

King, J.-R., Sitt, J. D., Faugeras, F., Rohaut, B., El Karoui, I., Cohen, L., Naccache, L., & Dehaene, S. (2013). Information sharing in the brain indexes consciousness in noncommunicative patients. *Current Biology: CB*, *23*(19), 1914–1919. https://doi.org/10.1016/j.cub.2013.07.075

Koch, C., Massimini, M., Boly, M., & Tononi, G. (2016). Neural correlates of consciousness: Progress and problems. *Nature Reviews. Neuroscience*, *17*(5), 307–321. https://doi.org/10.1038/nrn.2016.22

Laureys, S., Owen, A. M., & Schiff, N. D. (2004). Brain function in coma, vegetative state, and related disorders. *The Lancet. Neurology*, *3*(9), 537–546. https://doi.org/10.1016/S1474-4422(04)00852-X

Laureys, S., Celesia, G. G., Cohadon, F., Lavrijsen, J., León-Carrión, J., Sannita, W. G., Sazbon, L., Schmutzhard, E., von Wild, K. R., Zeman, A., & Dolce, G. (2010). Unresponsive wakefulness syndrome: A new name for the vegetative state or apallic syndrome. *BMC Medicine*, *8*. https://doi.org/10.1186/1741-7015-8-68

Lewis, L. D., Weiner, V. S., Mukamel, E. A., Donoghue, J. A., Eskandar, E. N., Madsen, J. R., Anderson, W. S., Hochberg, L. R., Cash, S. S., Brown, E. N., & Purdon, P. L. (2012). Rapid fragmentation of neuronal networks at the onset of propofol-induced unconsciousness. Proceedings of the National Academy of Sciences of the United States of America, 109(49), 19891. https://doi.org/10.1073/PNAS.1210907109

Luppi, A. I., Cabral, J., Cofre, R., Mediano, P. A. M., Rosas, F. E., Qureshi, A. Y., Kuceyeski, A., Tagliazucchi, E., Raimondo, F., Deco, G., Shine, J. M., Kringelbach, M. L., Orio, P., Ching, S., Sanz Perl, Y., Diringer, M. N., Stevens, R. D., & Sitt, J. D. (2023). Computational modelling in disorders of

consciousness: Closing the gap towards personalised models for restoring consciousness. *NeuroImage*, *275*, 120162. https://doi.org/10.1016/J.NEUROIMAGE.2023.120162

Madl, T., Baars, B. J., & Franklin, S. (2011). The Timing of the Cognitive Cycle. *PLoS ONE*, *6*(4). https://doi.org/10.1371/journal.pone.0014803

Mediano, P. A. M., Rosas, F. E., Luppi, A. I., Jensen, H. J., Seth, A. K., Barrett, A. B., Carhart-Harris, R. L., & Bor, D. (2022). Greater than the parts: a review of the information decomposition approach to causal emergence. Philosophical Transactions of the Royal Society A, 380(2227). https://doi.org/10.1098/RSTA.2021.0246

Naccache, L. (2018). Minimally conscious state or cortically mediated state? *Brain*, *141*(4), 949–960. https://doi.org/10.1093/brain/awx324

Owen, A. M., Coleman, M. R., Boly, M., Davis, M. H., Laureys, S., & Pickard, J. D. (2006). Detecting awareness in the vegetative state. *Science (New York, N.Y.)*, *313*(5792), 1402. https://doi.org/10.1126/SCIENCE.1130197

Peigneux, P. (2015). Neuroimaging Studies of Sleep and Memory in Humans, Curr Topics Behav Neurosci. https://doi.org/10.1007/7854_2014_326

Sanders, R. D., Tononi, G., Laureys, S., & Sleigh, J. W. (2012). Unresponsiveness ≠ unconsciousness. *Anesthesiology*, *116*(4), 946–959. https://doi.org/10.1097/ALN.0b013e318249d0a7

Schiff, N. D. (2015). Cognitive Motor Dissociation Following Severe Brain Injuries. *JAMA Neurology*, *72*(12), 1413–1415. https://doi.org/10.1001/JAMANEUROL.2015.2899

Schurger, A., Sarigiannidis, I., Naccache, L., Sitt, J. D., & Dehaene, S. (2015). Cortical activity is more stable when sensory stimuli are consciously perceived. *Proceedings of the National Academy of Sciences of the United States of America*, *112*(16), E2083-92. https://doi.org/10.1073/pnas.1418730112

Sergent, C., Faugeras, F., Rohaut, B., Perrin, F., Valente, M., Tallon-Baudry, C., Cohen, L., & Naccache, L. (2017). Multidimensional cognitive evaluation of patients with disorders of consciousness using EEG: A proof of concept study. *NeuroImage: Clinical*, *13*, 455–469. https://doi.org/10.1016/j.nicl.2016.12.004

Sitt, J. D., King, J.-R., El Karoui, I., Rohaut, B., Faugeras, F., Gramfort, A., Cohen, L., Sigman, M., Dehaene, S., & Naccache, L. (2014). Large scale screening of neural signatures of consciousness in patients in a vegetative or minimally conscious state. *Brain: A Journal of Neurology*, *137*(Pt 8), 2258–2270. https://doi.org/10.1093/brain/awu141

Song, C. and Tagliazucchi, E. (2020). Linking the nature and functions of sleep: insights from multimodal imaging of the sleeping brain. Current Opinion in Physiology. Elsevier Ltd, 15, pp. 29–36. https://doi.org/10.1016/j.cophys.2019.11.012

Stender, J., Gosseries, O., Bruno, M.-A., Charland-Verville, V., Vanhaudenhuyse, A., Demertzi, A., Chatelle, C., Thonnard, M., Thibaut, A., Heine, L., Soddu, A., Boly, M., Schnakers, C., Gjedde, A., & Laureys, S. (2014). Diagnostic precision of PET imaging and functional MRI in disorders of consciousness: A clinical validation study. *Lancet (London, England)*, *384*(9942), 514–522. https://doi.org/10.1016/S0140-6736(14)60042-8

Strauss, M., Sitt, J. D., King, J.-R., Elbaz, M., Azizi, L., Buiatti, M., Naccache, L., Wassenhove, V. van, & Dehaene, S. (2015). Disruption of hierarchical predictive coding during sleep. *Proceedings of the National Academy of Sciences*, *112*(11), E1353–E1362. https://doi.org/10.1073/pnas.1501026112

Strauss, M., Sitt, J. D., Naccache, L., & Raimondo, F. (2022). Predicting the loss of responsiveness when falling asleep in humans. NeuroImage, 251, 119003. https://doi.org/10.1016/J.NEUROIMAGE.2022.119003

Franklin S, Baars BJ, Ramamurthy U, Ventura M (2005). The Role of Consciousness in Memory. Brains, Minds and Media, Vol. 2005, bmm150.

Tsuchiya, N., Wilke, M., Frässle, S., & Lamme, V. A. F. (2015). No-Report Paradigms: Extracting the True Neural Correlates of Consciousness. *Trends in Cognitive Sciences*, *19*(12), 757–770. https://doi.org/10.1016/j.tics.2015.10.002

Türker, B., Musat, E. M., Chabani, E., Fonteix-Galet, A., Maranci, J.-B., Wattiez, N., Pouget, P., Sitt, J., Naccache, L., Arnulf, I., & Oudiette, D. (2023). Behavioral and brain responses to verbal stimuli reveal transient periods of cognitive integration of the external world during sleep. Nature Neuroscience 2023, 1–13. https://doi.org/10.1038/s41593-023-01449-7

Vinck, M., Uran, C., Spyropoulos, G., Onorato, I., Broggini, A. C., Schneider, M., & Canales-Johnson, A. (2023). Principles of large-scale neural interactions. *Neuron*, *111*(7), 987–1002. https://doi.org/10.1016/J.NEURON.2023.03.015

Wacongne, C., Labyt, E., Wassenhove, V. van, Bekinschtein, T., Naccache, L., & Dehaene, S. (2011). Evidence for a hierarchy of predictions and prediction errors in human cortex. *Proceedings of the National Academy of Sciences*, *108*(51), 20754–20759. https://doi.org/10.1073/pnas.1117807108

Welch, P. (1967). The use of fast Fourier transform for the estimation of power spectra: A method based on time averaging over short, modified periodograms. *IEEE Transactions on Audio and Electroacoustics*, *15*(2), 70–73. https://doi.org/10.1109/TAU.1967.1161901

Zelmann, R., Paulk, A. C., Tian, F., Villegas, G. A. B., Peralta, J. D., Crocker, B., Cosgrove, G. R., Richardson, R. M., Williams, Z. M., Dougherty, D. D., Purdon, P. L., & Cash, S. S. (2023). Differential cortical network engagement during states of un/consciousness in humans. Neuron, 111(21), 3479-3495.e6. https://doi.org/10.1016/J.NEURON.2023.08.007

Supplementary Materials

	State	Content	Content	State	Content
Markers	**VS_MCS**	**LS_LD**	**GS_GD**	**sleep_wake**	**unseen_seen**
Kolmogorov Complexity (KS)	0.355	0.732	1.1642E-09	3.815E-06	1
Permutation Entropy (PE) theta	8.222E-08	0.246	5.821E-09	4.768E-05	0.273
weighted Symbolic Mutual Information (wSMI) theta	7.998E-07	0.010	2.049E-08	0.001	1
Delta normalized	0.0003	7.942E-05	0.0002	9.537E-06	0.001
Theta normalized	3.235E-06	0.037	0.397	0.010	0.009
Alpha normalized	1.011E-08	0.0002	4.657E-10	3.624E-05	0.127
Beta normalized	1	0.035	2.314E-06	2.670E-05	0.002
Gamma normalized	1	0.227	2.328E-10	1.907E-06	0.005

Supplementary Table 1: p-values per marker of the Mann-Whitney and Wilcoxon statistical tests between the two distributions. All values are Bonferroni corrected for multiple tests (see Materials).

	State	Content	Content	State	Content
Markers	**VS_MCS**	**LS_LD**	**GS_GD**	**sleep_wake**	**unseen_seen**
Kolmogorov Complexity (KS)	0.559 (0.502, 0.616)	0.355 (0.227, 0.482)	0.016 (0.0, 0.043)	0.996 (0.981, 1.0)	0.395 (0.266, 0.54)
Permutation Entropy (PE) theta	0.668 (0.613, 0.723)	0.322 (0.212, 0.461)	0.038 (0.0, 0.101)	0.96 (0.881, 1.0)	0.323 (0.203, 0.458)
weighted Symbolic Mutual Information (wSMI) theta	0.656 (0.601, 0.709)	0.29 (0.183, 0.424)	0.12 (0.049, 0.215)	0.9 (0.777, 0.989)	0.514 (0.368, 0.642)
Delta normalized	0.38 (0.325, 0.437)	0.857 (0.761, 0.929)	1.0 (1.0, 1.0)	0.026 (0.0, 0.091)	0.825 (0.717, 0.913)
Theta normalized	0.649 (0.593, 0.702)	0.764 (0.653, 0.868)	0.684 (0.556, 0.814)	0.142 (0.04, 0.269)	0.806 (0.686, 0.896)
Alpha normalized	0.678 (0.623, 0.731)	0.188 (0.1, 0.301)	0.033 (0.002, 0.087)	0.947 (0.85, 1.0)	0.304 (0.186, 0.437)
Beta normalized	0.528 (0.471, 0.586)	0.243 (0.132, 0.357)	0.077 (0.014, 0.152)	0.977 (0.929, 1.0)	0.162 (0.077, 0.273)
Gamma normalized	0.481 (0.425, 0.54)	0.309 (0.18, 0.422)	0.149 (0.067, 0.252)	1.0 (1.0, 1.0)	0.193 (0.1, 0.307)

Supplementary Table 2: Area Under the Curve (AUC) values per condition and per marker with 0.95% confidence intervals (CI) calculated using 10,000 bootstrapped iterations. The format is AUC (lower bound CI, higher bound CI).

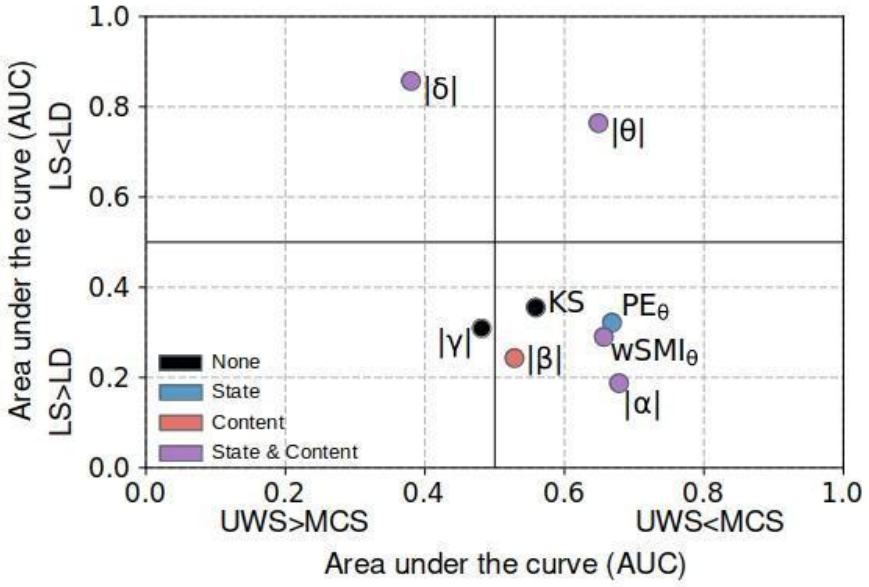

Supplementary Figure 1: Example #1, Behavior of EEG markers in the state and content dimensions for the auditory local-global dataset and disorders of consciousness patients. Each point represents in the x-axis the ability of the marker to discriminate between VS/UWS and MCS patients. In the y-axis, we represent the ability of the marker to discriminate between the local deviant and the local standard trials in the local-global paradigm. Note that the zero of the axes is centered at 0.5. An AUC of 0.5 corresponds to discrimination at the same level of chance. See the Methods for the marker abbreviations.

Author contributions

Pauline Perez: Conceptualization, Methodology, Software, Formal analysis, Investigation, Data curation, Writing - Original Draft, Visualization

Dragana Manasova: Methodology, Software, Formal analysis, Data curation, Writing - Original Draft, Writing - Review & Editing, Visualization

Bertrand Hermann: Investigation, Writing - Review & Editing.

Federico Raimondo: Software, Writing - Review & Editing

Benjamin Rohaut: Investigation, Writing - Review & Editing

Tristán A. Bekinschtein: Writing - Review & Editing, Funding acquisition.

Lionel Naccache: Writing - Review & Editing, Funding acquisition.

Anat Arzi: Investigation, Writing - Review & Editing, Visualization, Supervision

Jacobo D. Sitt: Conceptualization, Methodology, Writing - Review & Editing, Supervision, Project administration, Funding acquisition.

Acknowledgments

We would like to thank Mathias Michel for their help with the conceptualization of the study and for feedback on the manuscript. We thank all of the participants who took part in the studies. We would like to thank the work and support of the clinicians at the Neuro ICU, DMU Neurosciences, APHP- Sorbonne Université, Hôpital de la Pitié Salpêtrière, Paris, France; and the patient families whose consent and understanding are essential to the progress of the field.

This work was supported by the Ecole Doctorale Frontières de l'Innovation en Recherche et Education–Programme Bettencourt (to D.M.), by Sorbonne Université (to P.P.) and by a Marie Curie Individual Fellowship (840711 awarded to A.A.). This project is part of the multicentric application for the EU ERAPerMed Joint Translational Call for Proposals for "Personalised Medicine: Multidisciplinary research towards implementation" (ERA PerMed JTC2019). It is funded by local funding agencies of the participating countries (for France it is the Agence Nationale de Recherche ANR, funding code: ANR-19-PERM-0002). This project is supported by the Human Brain Project (HBP) MODELDxConsciousness Consortium (Agence Nationale de Recherche ANR, funding code: S.1600.ANR.HBPR). Preliminary ideas

of this work were presented in the NCC symposium on the 23th ASSC meeting (London Ontario 2019).

Statement of data availability

The data is not publically available.